Characterization of iron ore pellets by multimodal microscopy and image analysis

Reynel Martinez Castellanos

Doutorando

Universidade Federal do Rio de Janeiro - UFRJ

Programa de Engenharia Química (PEQ) - COPPE

Rio de Janeiro - Rio de Janeiro - Brasil

reynel.martinez@hotmail.com

Julio César Álvarez Iglesias

Pesquisador

Pontifícia Universidade Católica

do Rio de Janeiro (PUC-Rio)

Departamento de Engenharia Química e

de Materiais (DEQM)

Rio de Janeiro - Rio de Janeiro - Brasil

julioc.alvarez@gmail.com

Otávio da Fonseca Martins Gomes

Pesquisador

Centro de Tecnologia Mineral

Professor

Programa de Pós-Graduação em

Geociências Museu Nacional

Universidade Federal do Rio de Janeiro - UFRJ

Rio de Janeiro - Rio de Janeiro - Brasil

ogomes@gmail.com

Karen Soares Augusto

Pesquisadora

Pontifícia Universidade Católica

do Rio de Janeiro (PUC-Rio)

Departamento de Engenharia Química e

de Materiais (DEQM)

Rio de Janeiro - Rio de Janeiro - Brasil

karenaugusto@yahoo.com.br

Sidnei Paciornik

Professor-Associado

Pontifícia Universidade Católica

do Rio de Janeiro (PUC-Rio)

Departamento de Engenharia Química e

de Materiais (DEQM)

Rio de Janeiro - Rio de Janeiro - Brasil

sidnei@puc-rio.br

Abstract

A correlative approach employing optical microscopy and scanning electron microscopy is proposed for the quantification of phases and pores in iron ore pellets. Combining mosaic images covering the full cross-sections of pellets, obtained with both techniques, it is possible to improve the discrimination of pores, quartz and silicates. First, the images must be carefully registered to show the exact same regions. The procedure for registration, discrimination and quantification was developed with Fiji open source software. A qualitative and quantitative analysis confirmed the advantages of the correlative method as compared to the individual techniques.

Keywords: iron ore pellets; digital microscopy; multimodal microscopy; microstructural characterization; image analysis; Fiji; ImageJ.

1. Introduction

The importance of microstructural characterization techniques has increased in the mining and steel industries in order to assess and control the quality of iron ore and its agglomerates in terms of mineralogy, texture and porosity. It can provide key information to improve the iron ore beneficiation operations

and subsequent steelmaking process. In a joint research project between PUC-Rio and Vale SA, Brazil´s largest mining company, new methods based on digital optical microscopy and image analysis are being developed for the characterization of iron ore, sinters and pellets (Iglesias *et al.*, 2008; Wagner *et al.*, 2008; Gomes *et al.*, 2010; Iglesias *et al.*, 2011; Gomes *et al.*, 2013; Augusto *et al.*, 2015). These new methods reduced time consumption and operator dependency of characterization routines by automating some steps, such as image acquisition on the optical microscope, recognition of minerals, measurement of phase fractions, and determination of mineral texture and porosity. These techniques are the objects of two patents and they have been in current use in Vale´s laboratories for some years (Vieira *et al.*, 2015a and 2015b).

The main analytical technique used for the microstructural characterization of iron ore and its agglomerates is reflected light microscopy (RLM). The most common iron oxides and oxyhydroxides can be easily recognized by their reflectances. However, RLM is not able to differentiate all the phases present in iron ores, sinters and pellets, since transparent minerals and the embedding resin present similar

reflectance (Neumman and Stanley, 2008). It is a classical problem in ore microscopy that in fact became a challenge. Some authors, e.g. Delbem *et al.* (2015), proposed alternatives to address it, but their solutions are not consensually accepted mainly due to reproducibility limitations. On the other hand, scanning electron microscopy (SEM) is capable of discriminating quartz and other transparent minerals from the embedding resin, but it is not suitable to identify phases with close average atomic numbers with similar chemical composition, such as hematite and magnetite (Gomes and Paciornik, 2008). Donskoi *et al.* (2013) performed a comparative study of iron ore characterization using SEM and RLM. They basically concluded that although SEM systems can provide more detailed information on the gangue minerals, RLM is faster, more cost effective and more reliable for routine analysis of iron ores containing a variety of iron oxides and oxyhydroxides. In fact, a combined approach using both techniques may provide a comprehensive method for characterizing iron ores. A method to correlate images from RLM and SEM in order to enhance the SEM analytical capacity using reflectance (color) information was

developed by Gomes (2007). This method comprises co-localization of fields imaged in both microscopes, image registration involving rigid and non-rigid transformations and image analysis, allowing discrimination of phases that are indistinguishable in each single technique.

Some authors established semi-automatic procedures for the characterization of iron ore pellets through RLM and image analysis (IA), such as Wagner *et al.* (2008) and Nellros and Thurley (2011). These methods use an optical microscope with a motorized stage to perform step-wise displacements and acquire a large set of images in order to compose a mosaic (extended field) image covering an entire pellet. The mosaic image provides a useful overview of the whole pellet cross-section allowing qualitative and quantitative evaluation of the spatial distribution of porosity and phases.

This paper presents a multimodal microscopy method to discriminate and measure phases and pores in iron ore pellets. It combines mosaic images obtained with RLM and SEM in order to improve the discrimination of pores, quartz and silicates. The IA procedure was developed with Fiji open source software (Schindelin *et al.*, 2012).

2. Materials and methods

2.1 Sample preparation

The pellets were prepared at the Vale pelletizing plant in Vitória with iron ore from the Carajás mines. The approximately spherical samples were cut in half and embedded in epoxy resin. They were ground using diamond impregnated metal discs with 70 µm sized diamond particles,

followed by particle sizes 40, 15 and 6 µm. This roughing was carried out with water for 2 min for the first three particle sizes and 4 min for the last one.

After roughing, the samples went through an ultrasonic bath to remove any possible residues, and prevent any

scratching during polishing. The polishing steps used cloths with diamond suspensions of 3 and 1 µm for approximately 1 h each. Three different iron ore pellet samples were obtained, each with a highly polished 30 mm diameter section.

2.2 Digital microscopy

Two microscopes were used for image acquisition:

a) A Zeiss AxioImager.M2m computer-controlled optical microscope with a digital camera (Zeiss AxioCam MRc5 – 1292 x 968 pixels) was employed. The images were acquired using a 20X objective lens (EC Epiplan 20X/0.40) in the RGB mode, leading to a resolution of 0.53 µm/pixel.

b) A fully automated FEI Quanta 400 SEM with a backscattered electron detector was used. The images were acquired with 200X and 1000 x 1000 pixels, leading to a resolution of 1.23 µm/pixel.

For each pellet, sets of partially overlapping fields were imaged in both RLM and SEM in order to cover the entire sample cross-section. The overlap-

ping regions were used in an automatic correlation procedure to align adjacent field images. The mosaic covering the full cross section had 18822 x 19015 pixels in the RLM image and 9616 x 9214 pixels in the SEM image.

A reference mark in the sample was used to align it in the microscope sample holders and reduce the rotation error between acquisitions.

2.3 Image processing and analysis

All the processing and image analysis steps were performed in Fiji open source

software. These steps are described in the following section together with results.

3 Results and discussion

3.1 Alignment and registration of optical and SEM images

As the SEM pixel size is more than double the RLM pixel size, the first step was to interpolate pixels in the SEM image to match the digital resolution and allow further processing. Afterward, registration was performed automatically with the ImageJ plugin Linear Stack Alignment with SIFT (Saalfeld, 2008). This procedure detects homologous points in the two images with the SIFT method (Lowe, 2004) and uses these points in a spatial transformation to match point positions and register the images. In the present case, an Affine transformation (Zitova and Flusser, 2003) was used to correct translation, rotation, and residual resolution differences. After registration, it becomes possible to compare phase identification and quantification in both images.

3.2 Qualitative analysis with RLM

Once registered, the images were segmented to identify the phases present. In the RLM image (Figure 1a) the following phases were identified: hematite, quartz, other silicates and pores. Figure 1b shows the result of the segmentation using the following color code (cyan = pores, green = quartz, blue = silicates and red = hematite).

Figures 1c and 1d show a small area magnified. On analyzing these figures carefully (see arrows), one can conclude that some pores filled with resin or with internal reflection were incorrectly identified as quartz. Therefore, in RLM images, pores are underestimated while quartz is overestimated. However, the advantage of this technique is that it clearly differentiates the fine silicate particles from the pores, which is a problem in SEM images.
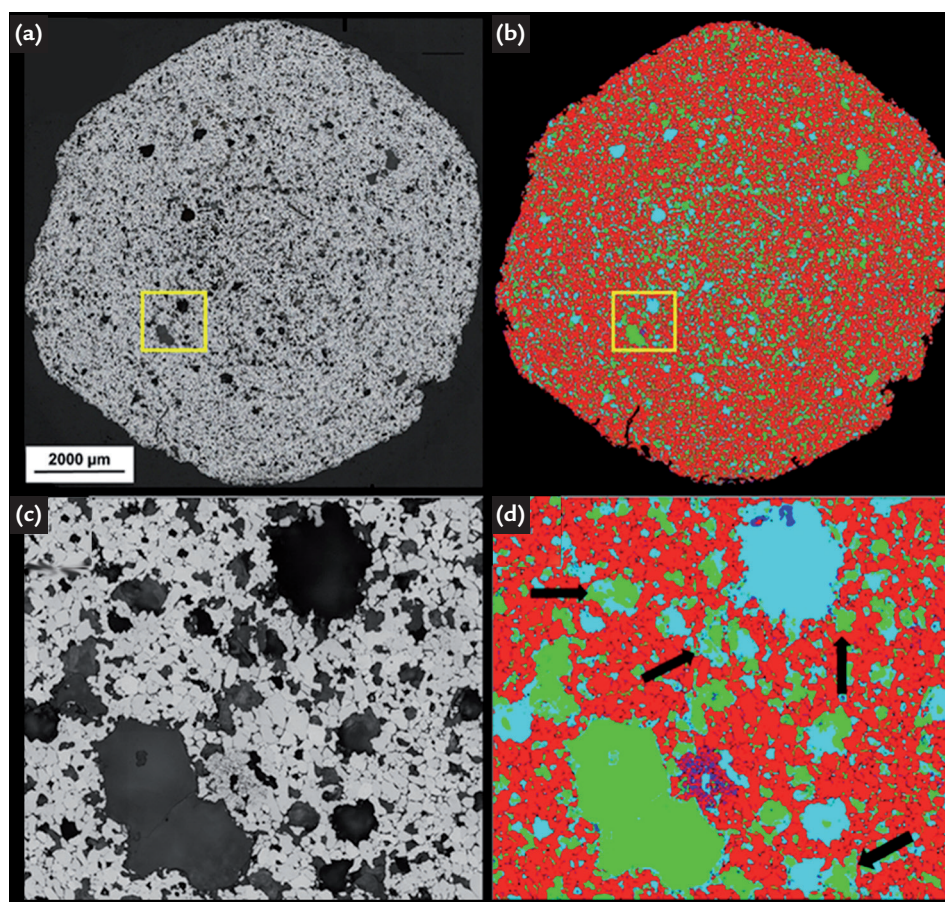

Figure 1
Segmentation of the phases in a RLM image: a) Original mosaic Image; b) Segmentation of the phases; c) Magnification of the yellow rectangle in (a); d) Magnification of the same region from (b): cyan = pores, green = quartz, blue = silicates and red = hematite. Arrows indicate the incorrect segmentation of pores with resin mistaken for quartz.

Although magnetite was not present in the samples used in this work, it is often present in ore pellets. However, the RLM technique can efficiently differentiate magnetite from hematite, which, on the other hand is quite difficult with SEM.

3.3 Qualitative analysis with SEM

Figure 2a shows the image obtained by SEM. Figure 2b shows the segmented image with the phases identified using the same color code as RLM. A magnification (Figure 2c) of the same region chosen in RLM image shows the characteristic details of each phase, which can be identified from their grey shades. Figure 2d shows that the SEM image segmentation separates quartz from the pores filled with resin, which usually appear mixed in RLM images. The disadvantage of this technique is that as SEM offers a greater depth of focus, the shallow pores that are not filled with resin may contain particles with intermediate shades that can be mistaken for other silicates. Thus, the pores are also underestimated, and in this case due to the overestimation of silicates. Hematite is correctly segmented, as it appears much brighter than the other phases. The possible confusion with magnetite does not happen as these samples don't contain this phase.
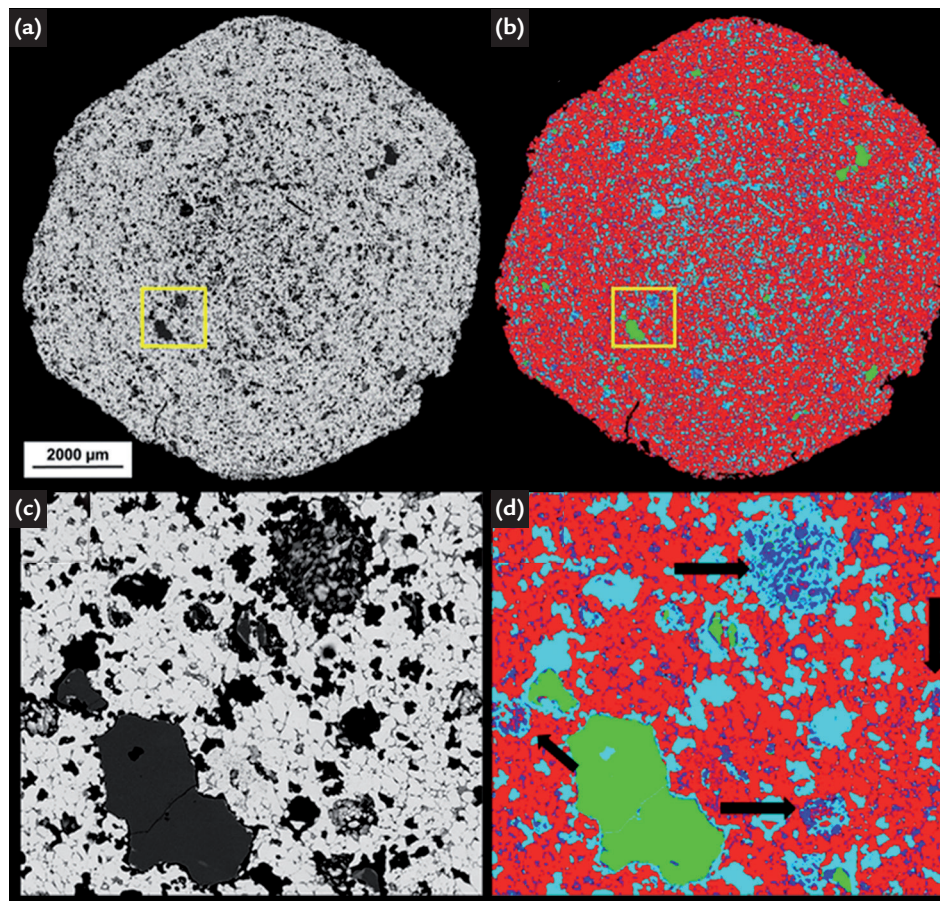
Figure 2
Segmentation of the phases in a SEM image: a) Original mosaic Image; b) Segmentation of the phases; c) Magnification of the yellow rectangle in (a); d) Magnification of the same region from (b): cyan = pores, green = quartz, blue = silicates and red = hematite. Arrows indicate the pores that are segmented as silicates.

3.4 Qualitative analysis using RLM and SEM correlated

After the separate segmentation of the phases in the RLM and SEM images separately, the correlation of the two techniques was performed. Here, the same images shown in the previous subsections obtained by RLM (IRLM Figure 3a) and by SEM (ISEM Figure 3b) were used.

The following symbols will be used in the quantitative analysis: P (pores), Q (quartz), S (silicates), (M) magnetite, H (hematite) with a subscript identifying the technique (RLM, SEM) or correlative (RLMSEM). Even though magnetite is not present in these samples, in general it must be considered. Hematite and magnetite are reliably obtained from RLM. Thus, M_{RLM} and H_{RLM} are accurate values. Quartz is reliably obtained from SEM,

QSEM is an accurate value. Segmentation generates binary images in which the phase of interest is displayed with white pixels against a black background. Thus, arithmetic and logic operations can be performed with these images. Now, the correct fraction of pores can be obtained by combining the results of the two techniques (Equations 1-5):

$$P_{RLMSEM} = (P_{RLM} \text{ OR } P_{SEM}) \qquad (1)$$

where OR represents the union operation. Subtracting image P_{RLMSEM} from image I_{SEM}, the solid phases are obtained:

$$I_{SEM} - P_{RLMSEM} = Q_{SEM} + S_{SEM} + (M_{SEM} + H_{SEM}) \qquad (2)$$

In the SEM images hematite and magnetite are segmented together, thus the use of the parentheses in the above expression. But the phases are correctly segmented in RLM, so that one can replace them in the above expression, as follows:

$$I_{SEM} - P_{RLMSEM} = Q_{SEM} + S_{SEM} + M_{RLM} + H_{RLM} \qquad (3)$$

Knowing that quartz (Q_{SEM}) is properly identified in the SEM image, it was also subtracted from this binary image:

$$I_{SEM} - P_{RLMSEM} - Q_{SEM} = S_{SEM} + M_{RLM} + H_{RLM} \qquad (4)$$

Finally, the silicates, which are the most difficult phase to discriminate in SEM, are correctly quantified (in the present samples $M_{RLM} = 0$):

$$S_{RLMSEM} = I_{SEM} - P_{RLMSEM} - Q_{SEM} - M_{RLM} - H_{RLM} \qquad (5)$$

The final segmentation result is shown Figure 3c using the same color code as before.
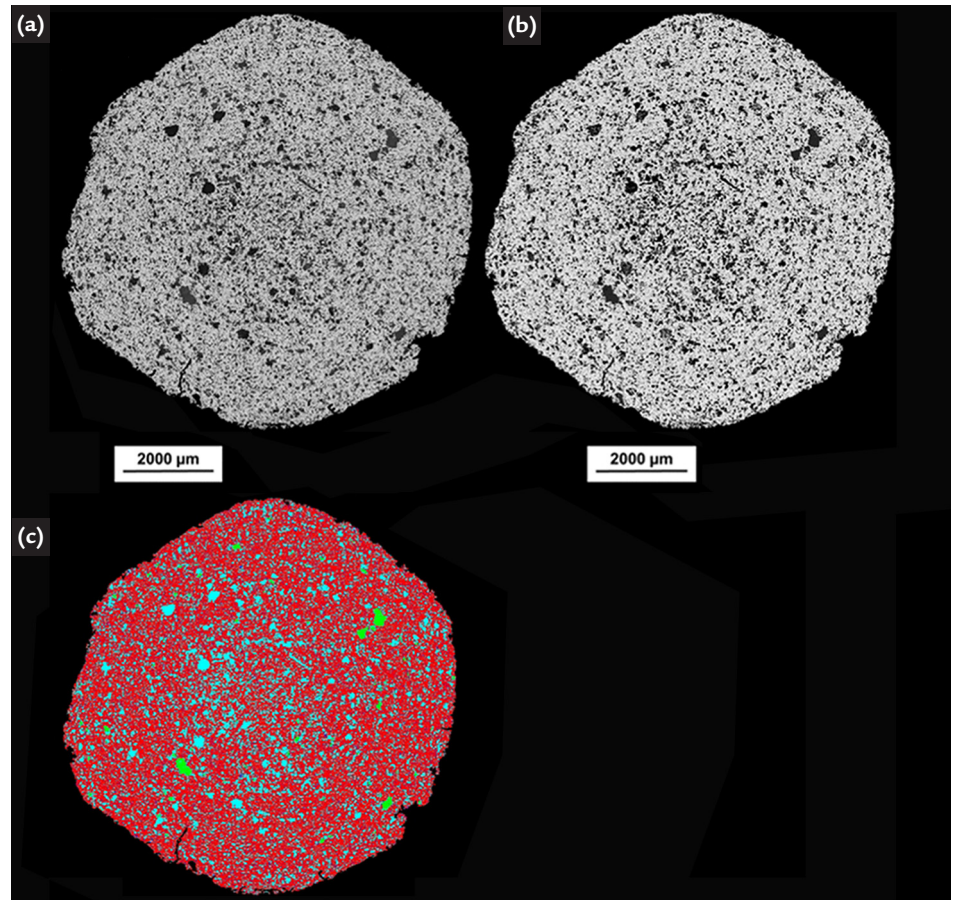

Figure 3
Correlation RLM + SEM: a) RLM image; b) SEM image; c) Correlation of the segmented phases: cyan = pores, green = quartz, blue = silicates and red = hematite.

Figure 4 shows the same magnified region as in the previous images. Figures 4a and 4b, correspond to the original RLM and SEM images, respectively. Figures 4c and 4d show the identification results of the phases obtained by each technique. The best phase discrimination is shown in Figure 4e with RLM+SEM correlated. Here we can clearly see that quartz and silicates are much better separated from the pores.
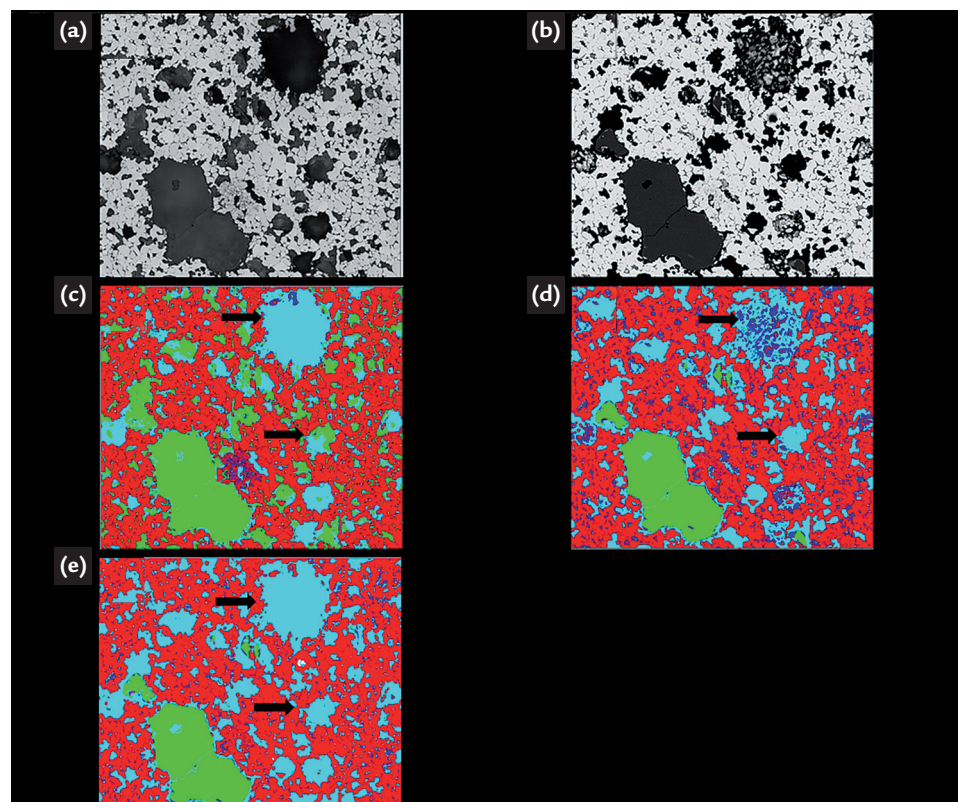

Figure 4
Magnified regions of the previous figures: a) Magnified region from RLM; b) Magnified region from SEM; c) Magnified region segmented, RLM; d) Magnified region segmented, SEM; e) Magnified region segmented and correlated (RLM + SEM). cyan = pores, green = quartz, blue = silicates and red = hematite. Arrows indicate the improvement in pore segmentation.

3.5 Quantitative analysis of results

Although the qualitative analysis has only shown the images of one pellet, in fact, in this study 3 iron ore pellets were analyzed. The different fractions of each of the phases present in the 3 pellets analyzed (P1, P2, P3) were quantified from RLM, SEM and the RLM + SEM correlative images using the exact same procedure. The results are shown in Figure 5.

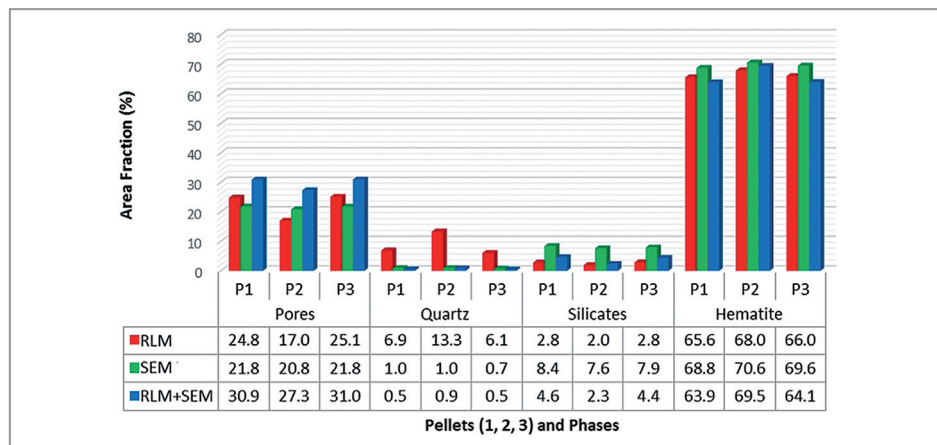|	Pores			Quartz			Silicates			Hematite		
	P1	P2	P3	P1	P2	P3	P1	P2	P3	P1	P2	P3
RLM	24.8	17.0	25.1	6.9	13.3	6.1	2.8	2.0	2.8	65.6	68.0	66.0
SEM	21.8	20.8	21.8	1.0	1.0	0.7	8.4	7.6	7.9	68.8	70.6	69.6
RLM+SEM	30.9	27.3	31.0	0.5	0.9	0.5	4.6	2.3	4.4	63.9	69.5	64.1

Figure 5
Phase fractions (%) for 3 iron ore pellets (P1, P2, P3) analyzed with the separate techniques (RLM and SEM) and their correlation (RLM + SEM).

These results support the qualitative analysis. The quartz fraction is higher in the 3 pellets measured by RLM, due to the fact that the pores filled with resin are misinterpreted as particles of quartz, underestimating the area of pores and overestimating the amount of quartz.

The silicate fractions are greater in the SEM images than in the RLM images. This is because shallow pores have been incorrectly segmented as silicates.

Therefore, in this technique the area of the pores is also underestimated and the silicates overestimated.

The pore fractions measured by the correlative technique are higher for the 3 pellets, showing the tendency of this technique to correct the underestimated pore values. In turn, the quartz areas are similar to those obtained in the segmentation of the SEM images, eliminating the overestimation of quartz from the RLM result. A similar correction of the silicates also takes place with the correlative technique.

The values found for hematite are similar for the 3 techniques for the 3 pellets. This phase does not present any problems of identification in either of the two techniques (for SEM because of the absence of magnetite, in this case) having a well-defined peak in the histogram, which facilitates its segmentation.

4. Conclusion

The phases present in the optical images of iron ore pellets can be identified due to their reflectance characteristics. However, the main problem of this technique lies in the limitation to differentiate the quartz from pores that are filled with resin. On the other hand, this technique correctly identifies the silicate regions without misidentifying them for pores as in the SEM technique. Also, if the iron ore contains magnetite then the optical technique can be used to discriminate it from hematite, since these two phases are hardly distinguishable with SEM.

The images obtained by SEM have the advantage of differentiating quartz correctly from the rest of the phases without creating confusion with the resin-filled pores. The disadvantage of this technique is that some pores can be misidentified as silicates, thus underestimating the porosity.

Both RLM and SEM have advantages and limitations. Correlating the two techniques to analyze the microstructure of a pellet provides better identification of the mineral phases and the pores with more accurate measurements than each of the techniques separately. This approach combines the advantages of both techniques providing results with a lower margin of error.

Acknowledgements

References

AUGUSTO, K. S., IGLESIAS, J. C. A., DURAND, L. D., GOMES, O. D. M., PIROTTE, D., DOMINGUES, A. L. A., VIEIRA, M. B., PACIORNIK, S. Automatic classification of hematite in iron ore. In: INTERNATIONAL CONGRESS FOR STEREOLOGY AND IMAGE ANALYSIS, 14. 2015. Liège. *Proceedings…* Prague: International Society for Stereology & Image Analysis, 2015.

DELBEM, I. D., GALÉRY, R., BRANDÃO, P. R. G., PERES, A. E. C. Semi-automated iron ore characterisation based on optical microscope analysis: quartz/resin classification. *Minerals Engineering,* v. 82, p. 2-13, 2015.

DONSKOI, E., MANUEL, J. R., AUSTIN, J. R., POLIAKOV, A., PETERSON, M.

J., HAPUGODA, S. Comparative study of iron ore characterisation using a scanning electron microscope and optical image analysis. *Trans. Inst. Min. Metall. (Sect. B: Appl. Earth Sci.),* v. 122, n. 4, p. 217-29, 2013.

GOMES, O. D. M. *Microscopia co-localizada: novas possibilidades na caracterização de minérios.* Rio de Janeiro: Catholic University of Rio de Janeiro (PUC-Rio), 2007. 2007. 103 p. (D.Sc. Thesis in Metallurgical and Materials Engineering in Portuguese).

GOMES, O. D. M., IGLESIAS, J. C. A., PACIORNIK, S., VIEIRA, M. B. Classification of hematite types in iron ores through circularly polarized light microscopy and image analysis. *Minerals Engineering,* v. 52, p. 191-7, 2013.

GOMES, O. D. M., PACIORNIK, S. Iron ore quantitative characterization through reflected light-scanning electron co-site microscopy. In: INTERNATIONAL CONGRESS ON APPLIED MINERALOGY, 9, 2008. Brisbane. *Proceedings…* Carlton: AusIMM, 2008. p. 699-702.

GOMES, O. D. M., PACIORNIK, S., IGLESIAS, J. C. A. A simple methodology for identifying hematite grains under polarized reflected light microscopy. In: INTERNATIONAL CONFERENCE ON SYSTEMS, SIGNALS AND IMAGE PROCESSING – IWSSIP, 17. 2010. Rio de Janeiro. *Proceedings…* Niterói: EdUFF, 2010. p. 428-31.

IGLESIAS, J. C. A., GOMES, O. D. M., PACIORNIK, S. Automatic recognition of hematite grains under polarized reflected light microscopy through image analysis. *Minerals Engineering,* v. 24, n. 12, p. 1264-70, 2011.

IGLESIAS, J. C. A., WAGNER, D. T., SCHINAZI, G., GOMES, O. D. M., MAURÍCIO, M. H. P., PACIORNIK, S., VIEIRA, M. B. Qualitative and quantitative evaluation of iron ore sinters through digital microscopy. In: INTERNATIONAL CONGRESS ON APPLIED MINERALOGY, 9, 2008. Brisbane. *Proceedings…* Carlton: AusIMM, 2008. p. 669-672.

LOWE, D. G. Distinctive image features from scale-invariant keypoints. *International Journal of Computer Vision,* v. 60, n. 2, p. 91-110, 2004.

NELLROS, F., THURLEY, M. J. Automated image analysis of iron-ore pellet structure using optical microscopy. *Minerals Engineering,* v. 24, n. 14, p. 1525-31, 2011.

NEUMANN, R., STANLEY, C. J. Specular reflectance data for quartz and some epoxy resins: implications for digital image analysis based on reflected light optical microscopy. In: INTERNATIONAL CONGRESS ON APPLIED MINERALOGY, 9, 2008. Brisbane. *Proceedings…* Carlton: AusIMM, 2008. p. 703-706.

SAALFELD, S. (2008). Linear Stack Alignment with SIFT. Available at: https://imagej.net/Linear_Stack_Alignment_with_SIFT

SCHINDELIN, J., ARGANDA-CARRERAS, I., FRISE, E., KAYNIG, V., LONGAIR, M., PIETZSCH, T., PREIBISCH, S., RUEDEN, C., SAALFELD, S., SCHMID, B., TINEVEZ, J. Y., WHITE, D. J., HARTENSTEIN, V., ELICEIRI, K., TOMANCAK, P., CARDONA, A. Fiji: an open-source platform for biological-image analysis. *Nature methods,* v. 9, n. 7, p. 676-82, 2012.

VIEIRA, M. B., PACIORNIK, S., GOMES, O. D. M., AUGUSTO, K. S., BORGES, A. A. M. *Automatic classification of the degree of maturation for iron ore pellets.* 2015a. (United States Patent 9207185).

VIEIRA, M. B., PACIORNIK, S., GOMES, O. D. M., IGLESIAS, J. C. A., BORGES, A. A. M. Automatic morphometry and classification of crystals of iron oxides. 2015b. (United States Patent 9121813).

WAGNER, D. T., ROUCO, H. V., GOMES, O. D. M., PACIORNIK, S., VIEIRA, M. B. Iron ore pellet characterization through digital microscopy. In: INTERNATIONAL SYMPOSIUM ON IRON ORE, 2. 2008. São Luís. *Annals…* São Paulo: ABM, 2008. p. 231-6.

ZITOVA, B., FLUSSER, J. Image registration methods: a survey. *Image and Vision Computing,* v. 21, n. 11, p. 977-1000, 2003.